CR-2-191

MORNING VEHICLE-START EFFECTS ON PHOTOCHEMICAL SMOG

June 1971

J. R. Martinez

R. A. Nordsieck

A. Q. Eschenroeder

Prepared for
Environmental Protection Agency
Air Pollution Control Office
Under Contract No. EHSD 71-22

GENERAL RESEARCH CORPORATION

P.O BOX 3587, SANTA BARBARA, CALIFORNIA 93105

In addition to approval by the Project Leader and Department Head, General Research Corporation reports are subject to independent review by a staff member not connected with the project. This report was reviewed by J. R. Brennand, Jr.

The work upon which this publication is based was pursuant to Contract No. EHSD 71-22 with the National Air Pollution Control Administration, Environmental Health Service, Public Health Service, Department of Health, Education and Welfare.

CR-2-191

MORNING VEHICLE-START EFFECTS ON PHOTOCHEMICAL SMOG

Contract No. EHSD-71-22

June 1971

J. R. Martinez

R. A. Nordsieck

A. Q. Eschenroeder

ABSTRACT

The influence of cold-start vehicle emissions on air quality is investigated using the General Research Corporation photochemical/diffusion model. Both the time and space distribution of cold starts are examined. A day from an October 1968 Los Angeles smog episode serves as a baseline for determining diffusion coefficients, nitrogen balance, and hydrocarbon reactivities. Vehicular and stationary sources for 1968, 1971, 1974 and 1980 are emission inputs, and pollutant concentrations at the ground are air quality outputs. Stagnant central basin conditions govern the time phasing studies.

Emissions introduced during the starting process have the greatest effect of all on carbon monoxide peaks, the effect being to increase the peak CO concentration from 9 to 13 percent. The levels of ozone and nitrogen dioxide that build up later in the day are influenced less because chemical processes afford dilution time. Thus for ozone the increase in concentration due to morning emissions ranges from 1 to 7 percent and for nitrogen dioxide the range is from 0 to 2 percent. Typical west-to-east morning air movement forms a background for the geographical distribution studies. If vehicle starts are decentralized geographically, only a slight increase in the pollutant loading is noted because of the low morning wind speeds. This increase is so small as to be insignificant compared with the starting emission portion of the total emissions. Based on the results of the study, three possible weighting schemes are proposed for combining cold-start and hot-start driving cycle measurements, each related to morning cold-start emissions.

CONTENTS

ILLUSTRATIONS

TABLES

I. INTRODUCTION

A. BACKGROUND OF THE PROBLEM

Time-phasing of pollutant emissions might exert a powerful influence on air quality in the case of photochemical smog. During the morning hours this is possible because on most days a period of atmospheric stability and stagnation is followed by a rising trend of solar radiation input.

Many of the analyses of motor vehicle air pollution contributions allocate emissions in direct proportion to car-miles per hour or traffic intensities. However, suboptimum fuel mixture conditions during the vehicle-start phase increase some of the emission rates above those for normal operating activities. The increases are larger for those starts occurring when the vehicle engine is not warm. Therefore, the morning starting contributions are especially significant since most of the vehicle population is subjected to startup (about 90% of them between 6 and 9 A.M. in Los Angeles[1]) and most of them have been idle for several hours preceding the start.

This becomes a key issue in the design of control system certification tests because the cold start is a relatively infrequent phenomenon and running emissions are continuously distributed. Because of the nature of the morning time-phasing, it may be that a uniform proration of starting emissions over the whole day's activities is not an adequate criterion for evaluating a control system. Consequently an analysis of the time-phasing effects is necessary to assess the cause/effect relationship between start-up contributions and air quality. Then the results of the analysis must be translated into a weighting scheme for combining the results of cold-start cycle and hot-start cycle tests for evaluating the performance of proposed control schemes.

B. OBJECTIVES OF THIS WORK

In this report, the relative importance of morning cold-start emissions is assessed for those effects associated with photochemical smog. A computer simulation model is used with aerometric data from the Los Angeles basin to study the buildup of air pollution as it is affected by starting emissions. The procedure relates meteorological factors, time/space traffic distributions, and ultraviolet solar radiation with the photochemical atmospheric mechanisms involved in air pollution. (Averaging over the daily activities of motor vehicles may not give an adequate description of the most severe conditions.)

Using validated input values and chemical parameters, we set out to determine air quality changes that are ascribable to vehicle start-up. The first step in the investigation is a determination of the source emission inventory for stationary and mobile emitters. Peculiar to our purpose is the segregation of the temporal and geographical distribution of starting contributions from the running emission distributions. Then, selecting a stagnant day in the Los Angeles basin we artificially remove these contributions to assess their effect on air quality. This is done for 1968, 1971, 1974, and 1980.

After the source characterization, the diffusion coefficient (as a function of time and height) is found for the central basin using measurements of meteorological conditions and carbon monoxide from late 1968. Uptake of nitrogen oxides by the ground, by urban surfaces, and by airborne particulates is not well known (in fact, it is a subject of active research). Consequently, the nitrogen balance near the ground is established as the next preparatory step in the investigation. Previously determined[2] reduction factors in the nitric oxide emissions are reconfirmed to account for the heterogeneous effects. Gas phase removal mechanisms are included, as shown in our last report,[3] and recently reported results[4] for NO_3 chains are added to update the model. Hydrocarbon reactivity is scaled down, as before, from the relatively high values characteristic of

propylene photo-oxidations to those characteristic of the aggregation of atmospheric hydrocarbons.

C. STUDY DESIGN

In an attempt to capture realism, all our simulation results include appropriate stationary source emissions as well as mobile source emissions constructed from vehicle age distributions. In keeping with the use of a stagnant slab model to approximate the central basin, we selected a baseline day with little wind, resulting in relatively high pollution. For the geographical distribution studies, we used average September wind patterns in the moving air parcel simulation. Four test years were chosen, some to make best use of the existing data base and others to reflect substantial changes in emission control systems.

Successive sections describe the modeling of source emission distribution, the choices of chemical model and baseline case, and the simulation results. The final section contains some overall observations and cautions regarding the results. It concludes with some suggestions for alternate weighting factors for cold- vs hot-start test cycle results.

II. SOURCE EMISSION DISTRIBUTION

In general, contaminant source emissions are distributed in space and time in a rather complex manner. The model of geographical and hourly variations used here is based largely on the work of Roberts, Roth, and Nelson.[5] The SDC driving patterns survey[1] provided a means for estimating the magnitude and temporal distribution of the morning start-up phenomenon, but the geographical distribution was chosen somewhat arbitrarily for lack of readily usable data. Annual variations in average daily source emissions, resulting from urban population growth and the increasing number of vehicles with various levels of emission control devices, were drawn from projections by the California Air Resources Board (ARB)[6] and the Los Angeles Air Pollution Control District (LAAPCD),[7] and from available test data,[8] standards, and surveys.[9]

A. MOTOR VEHICLE EMISSIONS

1. Average Annual Vehicle Emission Factors

Table 1 shows recent test data from Huls[8] for vehicle emission factors as measured on the new federal driving cycle,[10] with and without an initial cold-start. The tabulated differences, multiplied by 7.45 miles (the distance that would be covered during one federal cycle), provide baseline values of average grams per cold start for the five model years shown.

Lacking measured emission factors for other model years, we chose to use federal standards where available and "scale" California standards and pre-standard estimates to the federal cycle to fill in any remaining gaps between 1960 and 1975. Pre-1960 emission factors were assumed to be constant at the 1960 levels, and similarly, the 1975 emission factors were extrapolated as constant for all subsequent years. The scaling technique used is based on California ARB calculations of "equivalent standards" for 1972 under the new federal procedure.[11] Table 2 is reproduced from Ref. 11.

Sec. II A
Tables 1, 2

TABLE 1

FEDERAL CYCLE GRAM-PER-MILE EMISSIONS

BASED ON MEASUREMENTS (From Ref. 8)

Model Year		NO_x (as NO_2)	HC	CO
1968	Cold Start	6.11	4.80	71.34
(6 tests)	Hot Start	5.35	3.36	37.23
	Difference	0.76	1.44	34.11
1969	Cold Start	5.28	4.79	48.14
(54 tests)	Hot Start	4.40	3.51	28.87
	Difference	0.88	1.28	19.27
1970	Cold Start	6.18	4.11	41.91
(57 tests)	Hot Start	5.39	2.65	22.67
	Difference	0.79	1.46	19.24
1971	Cold Start	4.43	3.63	42.08
(25 tests)	Hot Start	3.71	2.80	29.66
	Difference	0.72	0.83	12.42
1975*	Cold Start	0.85	0.61	6.68
(3 tests)	Hot Start	0.99	0.25	0.90
	Difference	-0.14	0.36	5.78

*These three tests were carried out on 1971 model cars equipped with prototype versions of the emission control devices which are to be used on 1975 production models.

TABLE 2

EQUIVALENT CALIFORNIA AND FEDERAL EMISSION STANDARDS

Pollutant	California 1972 Standards	Equivalent New Procedure	Federal 1972 Standards
HC	1.5 gm/mi	3.2 gm/mi	3.4 gm/mi
CO	23 gm/mi	47 gm/mi	39 gm/mi

Based on these data, the scale factors 3.2/1.5 and 47/23 were used (where necessary) to convert California Standards and pre-standard estimates for HC and CO emissions to equivalent federal emission factors. NO_x emissions must be scaled slightly differently since the current federal test procedure does not provide for their measurement. To fill this gap, California has augmented the procedure by requiring that the federal test cycle be followed by two hot 7-mode (California) cycles for nitrogen oxides testing. The new equivalent 1972 standard under this procedure is 3.2 gm/mi NO_x as compared to 3.0 gm/mi under the 7-mode test procedure alone.[11] Hence, the scale factor 3.2/3.0 was used to convert NO_x emissions based on California cycle testing to their equivalent federal values. Once scaled, all emission factors were assumed to contain the effect of one cold-start as specified in the federal procedure.

To summarize, pre-1968 emission factors were obtained by the scaling technique, measured emissions data were used for the years 1968 through 1971 and for 1975, and the more stringent of the scaled California Standards or the Federal Standards were used for the years 1972, 1973 and 1974.

Given data for the contributions of cold-start emission factor for the model years shown in Table 1, we extrapolated back from 1968 and forward from 1975 assuming constant levels to obtain estimates of cold-start contributions to emission factors in other years. Between 1971 and 1975, the cold-start differentials were assumed to scale down in proportion to changes in exhaust emission standards in the intervening years. We then subtracted these cold-start contributions from the scaled federal-cycle emission factors to yield estimates of "hot-running" emission factors for the years not included in the test data.

Table 3 summarizes the "hot-running" emission factors and cold-start emissions used in the study. (As mentioned above, the gram-per-start cold-start emissions are obtained by multiplying the gram-per-mile cold-start differentials by 7.45 miles.) The 2.69 gram/mile evaporative

TABLE 3

HOT-RUNNING AND COLD-START EMISSIONS BY MODEL YEAR

Model Year	Hot-Running Emissions (grams/mile)			Cold-Start Emissions (grams/start)		
	NO_x (as NO_2)	HC	CO	NO_x (as NO_2)	HC	CO
1960 and before	3.50 (B)	22 06 (B) 2 69 evap. 4 10 blowby	128 9 (B)	5 66	10 73	254 1
1961	3 50 (B)	22 06 (B) 2 69 evap 4.10 blowby	128 9 (B)	5.66	10 73	254 1
1962	3.50 (B)	22.06 (B) 2 69 evap	128.9 (B)	5 66	10 73	254 1
1963	3 50 (B)	22 06 (B) 2 69 evap.	128 9 (B)	5 66	10 73	254 1
1964	3.50 (B)	22 06 (B) 2.69 evap	128 9 (B)	5.66	10 73	254 1
1965	3 50 (B)	22 06 (B) 2.69 evap.	128 9 (B)	5 66	10.73	254 1
1966	5.64 (B)	5 81 (B) 2 69 evap.	35 39 (B)	5 66	10 73	254.1
1967	5.64 (B)	5.81 (B) 2 69 evap.	35.39 (B)	5 66	10 73	254 1
1968	5.35 (A)	3 36 (A) 2 69 evap	37 23 (A)	5.66 (A)	10 73 (A)	254.1 (A)
1969	4.40 (A)	3.51 (A) 2.69 evap.	28 87 (A)	6 56 (A)	9 54 (A)	143 6 (A)
1970	5 39 (A)	2.65 (A) 2.69 evap.	22.67 (A)	5.89 (A)	10 88 (A)	143 3 (A)
1971	3.71 (A)	2.80 (A)	29.66 (A)	5 36 (A)	6.18 (A)	92.53 (A)
1972	2.66 (B)	2.63 (B)	28 70 (C)	4 02 (D)	4 25 (D)	76 74 (D)
1973	2 49 (C)	2.63 (B)	28 70 (C)	3 78 (D)	4 25 (D)	76 74 (D)
1974	2.49 (C)	2 63 (B)	28 70 (C)	3 78 (D)	4 25 (D)	76 74 (D)
1975 and after	0.99 (A)	0 25 (A)	0.90 (A)	-1 04 (E)	2 68 (A)	43 06 (A)

(A) Test data (see Table 1).[8]

(B) Obtained by scaling California Standard or estimate of pre-standard emission factor to federal test procedure[11] and subtracting cold-start contribution as extrapolated from test data (see text)

(C) Obtained by subtracting cold-start contribution from Federal Standard

(D) Lacking data in the 1972-1974 time period, it was assumed that the techniques employed to meet the standards used in obtaining the running emission factors (See (B) or (C) above) would act proportionally in scaling the cold-start emissions down from their 1971 values toward their 1975 values.

(E) Test data. The negative correction is always used in conjunction with the running emission factor, thereby reducing each post-1975 car's net NO_x contribution to the level predicted for a federal cycle with one cold-start, followed by hot-running emissions

emission factor shown in Table 3 for pre-1971 cars was calculated from data in Ref. 12 by assuming an average gasoline Reid vapor pressure of 8.5 lb/in^2, a Los Angeles County auto population of 3.95×10^6 cars,[7] and an average annual mileage of 10,000 miles per car. The result is in good agreement with Ref. 9. The evaporative emission controls introduced on 1971 and later cars were assumed to perform as specified. Blowby emissions on pre-1962 cars were set at 4.1 grams/mile[9] and were likewise assumed to be eliminated on post-1961 cars by the introduction of positive crankcase ventilation systems.

The model year emission factors in Table 3 were then combined in accordance with a vehicle age and usage distribution[13] shown in Table 4 to yield weighted average vehicle emission factors for each year to be analyzed. The resulting average running and cold-start emissions for 1968, 1971, 1974, and 1980 are shown in Table 5.

TABLE 4

VEHICLE AGE AND USAGE DISTRIBUTION AT CLOSE OF MODEL YEAR*
(From Ref. 13)

Age (years)	Fraction of Population	Miles Driven in Last Year
1	0.108	15,000
2	0.105	13,000
3	0.102	11,000
4	0.098	9,600
5	0.093	8,400
6	0.088	7,000
7	0.081	5,300
8	0.072	5,000
9	0.062	4,400
10	0.051	4,200
over 10	0.140	3,500

*Based on a survey of California vehicles stopped at California Highway Patrol roadside inspection stations.

TABLE 5

AVERAGE VEHICLE EMISSION FACTORS

Year	Hot-Running Emissions (grams/mile)			Cold-Start Emissions (grams/start)		
	NO_x (as NO_2)	HC	CO	NO_x (as NO_2)	HC	CO
1968	4.51	16.81	82.49	5.66	10.73	254.10
1971	4.55	10.00	51.58	5.76	9.69	188.71
1974	3.55	5.70	37.80	4.81	6.89	128.05
1980	1.52	0.93	6.55	0.17	3.46	54.69

2. Geographical Distribution

Using an extensive data base of traffic counts in the Los Angeles area, Roberts, Roth and Nelson, of Systems Applications, Inc. (SAI),[5] have characterized the spatial distribution of Los Angeles freeway and surface street traffic intensities in each of 625 grid squares of 2 × 2 miles each. Average daily traffic intensity within each square is represented by an estimate of the total number of vehicle miles (either freeway or non-freeway) driven in that square. As an example, Fig. 1 shows the resulting spatial distribution of freeway traffic used in the study (where the numbers in the squares are thousands of vehicle miles per day). A similar but more completely filled grid represents surface street traffic. The absolute traffic intensities given by SAI were assumed to apply as of 1968.

Two geographical distributions of the total "pulse" of cold-start emissions were used. For the stagnant slab-model, we assumed that morning start-ups were distributed uniformly, using the area of the Los Angeles Basin (1250 sq mi) [7] as an estimate of the size of the densely populated region. One of the primary purposes of analyzing a cross-basin trajectory

Sec. II A
Fig. 1

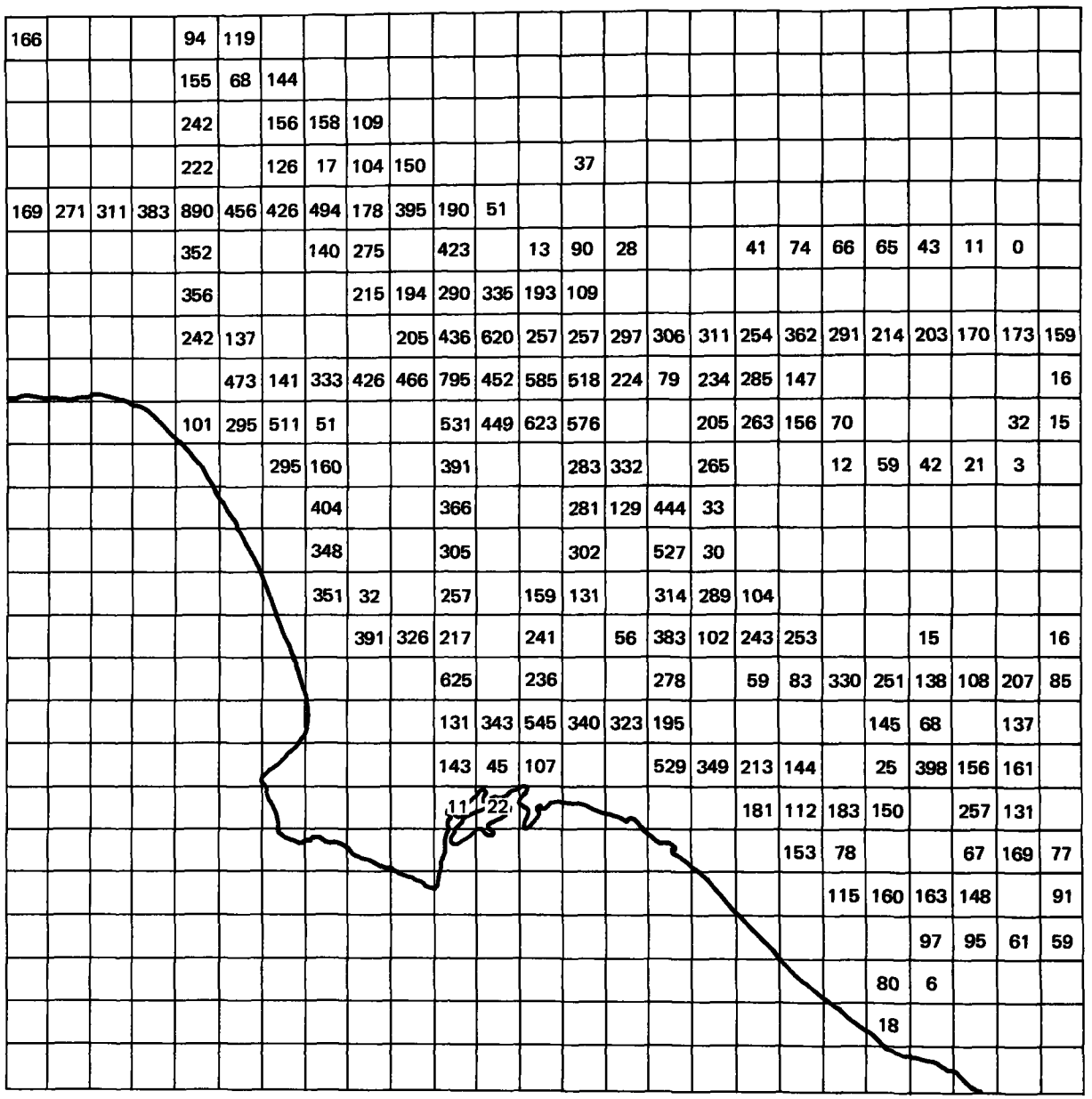

Figure 1. Geographical Distribution of Freeway Traffic in the Los Angeles Basin Area (Adapted from Roberts, Roth and Nelson, Ref. 5).

was to evaluate the effect of a more suburb-oriented cold-start distribution. Hence, for that case, we modeled both the uniform cold-start distribution and one in which the density of morning start-ups (essentially equatable to car residence density) was assumed to be 3 times as high at the outer edge of the populated area as in the basin center (here taken as the Federal building downtown), varying linearly in between.

3. Temporal Distribution

The hourly distributions of average daily traffic intensities for freeway and non-freeway traffic used in the study were those developed by SAI in conjunction with the geographical distributions described above. In their report,[5] SAI shows that only small errors are incurred by characterizing all freeway traffic by one time distribution and all non-freeway traffic by another. The resulting traffic/time distributions used to time-allocate the freeway and non-freeway mileages in each grid square are shown in Fig. 2.

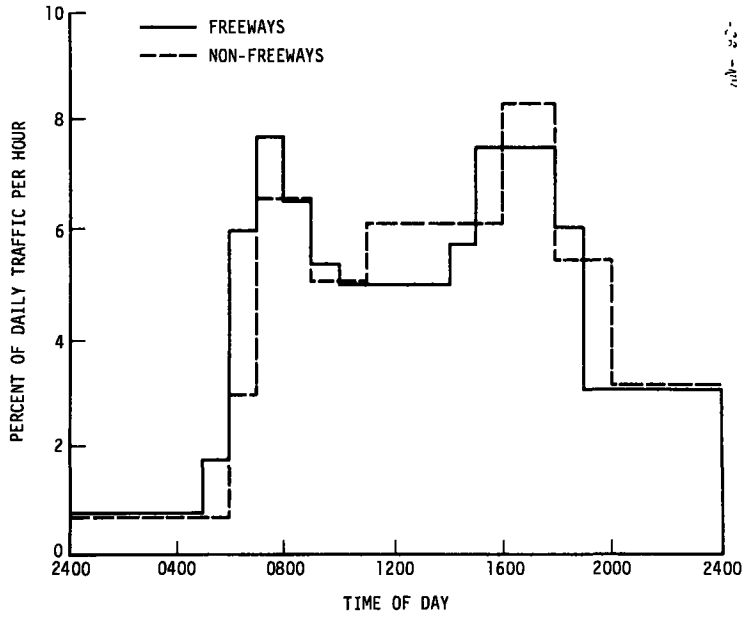

Figure 2. Los Angeles Traffic/Time Distributions (Adapted from Roberts, Roth and Nelson, Ref. 5)

Data reported by Systems Development Corporation (SDC)[1] on the distribution of weekday trip start times in Los Angeles indicates that the temporal distribution of morning car-starts can reasonably be approximated by a triangular pulse. The model selected starts from zero at 6:00 A.M., rises linearly to a peak at 7:30 A.M. and then falls linearly back to zero at 9:00 A.M. SDC's data also showed that of an average 4.4 trips per car weekday (in Los Angeles), 20.6% or 0.907 trips per car weekday were started between 6:00 and 9:00 A.M. Thus about 91% of the registered automobiles in L.A. County were assumed to contribute one morning start to the cold-start contaminant pulse.

Annual variations of total pollutant emissions from motor vehicles were assumed to grow in proportion to the registered vehicle population. Hence, based on an extrapolation of vehicle registration in L.A. County by the LAAPCD[7] and using 1968 as the baseline case, the vehicle mileages in each square of the geographical distributions were increased accordingly for each year analyzed beyond 1968. Of course, the cold-start contaminant pulse was similarly scaled up.

B. STATIONARY SOURCE EMISSIONS

The stationary source emissions modeled for this study included oxides of nitrogen and reactive hydrocarbons as characterized by SAI in Ref. 5. Stationary carbon monoxide emissions were neglected in comparison with motor vehicle CO emissions. The SAI model uses the same 25 × 25 grid of 2 × 2 squares described above to provide geographic source distribution. Within each square, the flux is given in kilograms per hour and is assumed to be constant between 6:00 A.M. and 6:00 P.M. This data was assumed to be circa 1968, and subsequent annual growth was modeled on the basis of ARB projections for the South Coast Air Basin.[6] Reference 6 shows negligible expected changes in total stationary hydrocarbon fluxes over the next 20 years; Figure 3 shows the growth curve obtained for stationary source NO_x emissions. These factors were used to increase the kilogram-per-hour NO_x fluxes in each grid square.

Sec. II C
Fig. 3

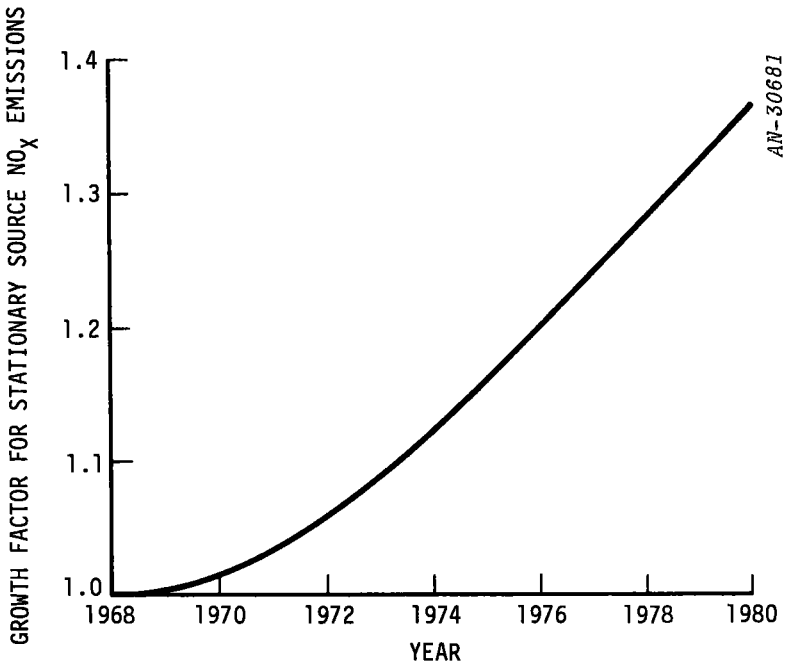

Figure 3. Estimated Growth of Stationary Source NO_x Emissions (From Ref. 6)

C. INPUT GENERATION FOR PHOTOCHEMICAL MODEL

1. Central Basin Stagnant Case

The character of the central basin stagnant mixing case is such that it would seem inappropriate to simply use the source data specified for the single 4-square-mile grid square containing the central basin measurement station.[14] Instead, to simulate more extensive local mixing during the eight-hour period of interest, source emission fluxes in neighboring grid squares were combined in an area-weighted average to yield an input flux history which represents an average over a 5 × 5 mile square centered on the measurement station.

2. Cross-Basin Trajectory Case

The Lagrangian air parcel formulation used in the current GRC model has been described in a previous report.[3] The air trajectory data

necessary to determine the schedule of changes in pollutant fluxes into the air parcel on a realistic cross-basin trajectory was obtained from Ref. 14. Figure 4 shows the trajectory, which was obtained from a combination of average September wind speeds and directions measured at stations near the coast, where the trajectory starts, and downtown at the Federal building, where the trajectory passes at about noon. The afternoon portion of the trajectory was obtained by estimating wind speeds and directions from a similar trajectory in Ref. 14. The resulting trajectory is very similar in path and time history to one constructed in Ref. 14 by more detailed analysis of average hourly resultant wind streamlines for September, and is therefore considered to be a realistic cross-basin air trajectory. Because the wind speeds near the coast are practically zero early in the morning, the trajectory shows no appreciable movement until after 8:00 A.M. As the air parcel subsequently moves along the trajectory, the schedule of pollutant influxes is determined by both the geographical and temporal source distributions described above.

Sec. II C
Fig. 4

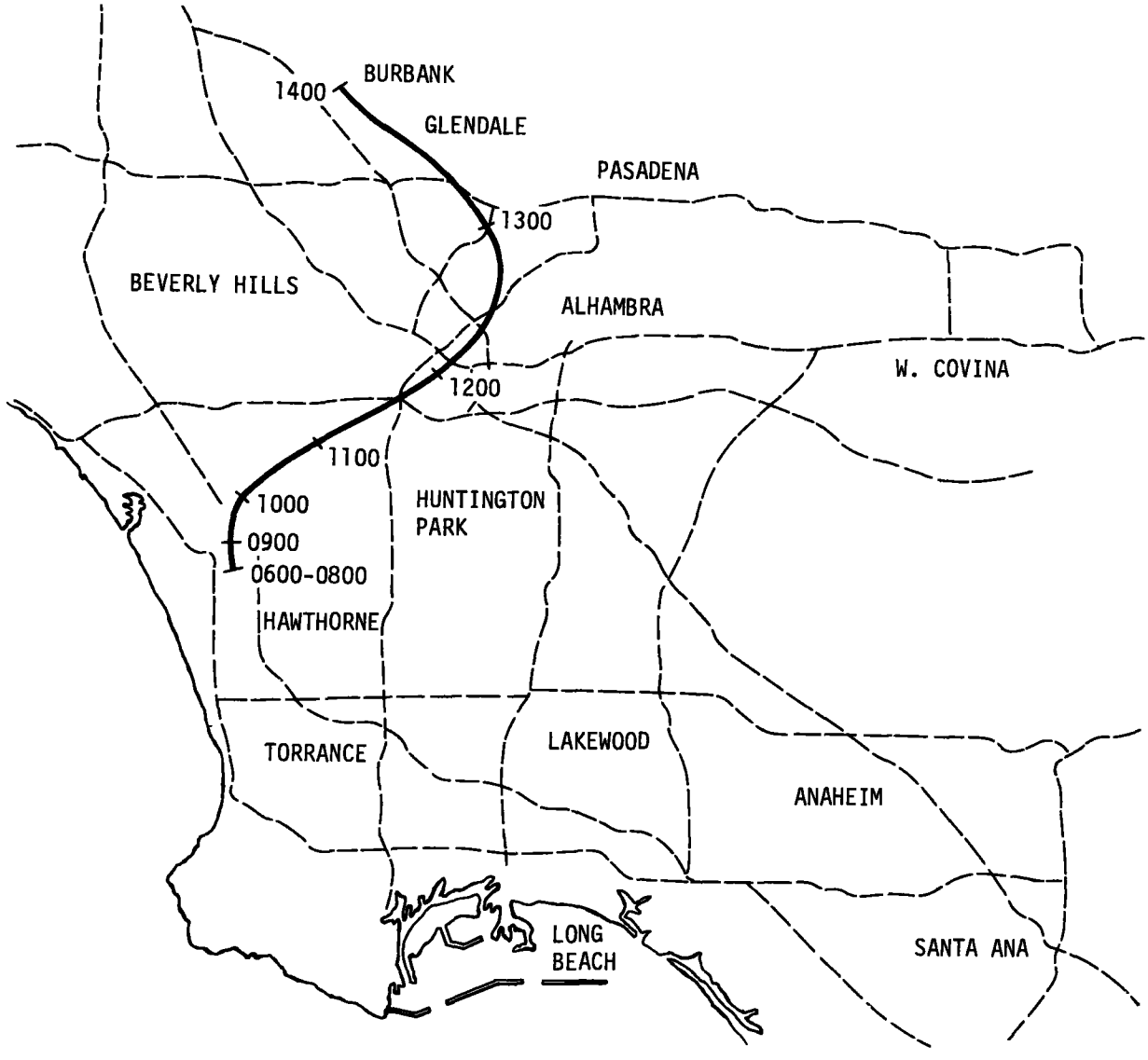

Figure 4. Cross-Basin Air Trajectory

III. CHOICES OF CHEMICAL MODEL AND BASELINE CASE

A. INCORPORATION OF NO_3 IN KINETICS

The basic 12-step kinetic model has been described in detail in Ref. 3. Table 6 shows the reactions and rate constants included in this version of the model.

One problem with the 12-step model was that late in the reaction the ozone and NO_2 concentrations were high. Although comparison with the measurements of Altshuller, et al[15] showed the computed ozone and NO_2 to be within the range of experimental uncertainty, validation of the model against atmospheric data[3,16] showed that the disparity can become large even after reducing the hydrocarbon rate constants. The kinetic scheme has now been modified in order to remedy this deficiency and thus achieves a higher degree of realism. The modifications are described below.

Two reactions and one species, NO_3, have been added to the kinetic model. These are shown as reactions 13 and 14 in Table 6. The $O_3 + NO_2$ reaction, shown in Table 6 as reaction 13, describes the late-time phenomena which lower the concentrations of ozone and NO_2. Tests of a mechanism with the addition of reaction 13 alone displayed anomalously high concentrations of RO_2 late in the reaction. This problem was solved by adding an $RO_2 + NO_3$ chainbreaking reaction (No. 14 in Table 6) following Hanst's[4] suggestion concerning the role of NO_3 in the formation of PAN. The rate constant assigned to reaction 14 is the same as that of reaction 7 since these two reactions are analogous.

The results of the simulation compared with experimental data for a propylene-nitrogen oxide system are shown in Figs. 5 and 6. The effect of the modifications is to lower the concentration of ozone and NO_2 late in the process. The production of PAN satisfies the criteria set forth by Hanst.[4] The effect that varying the initial NO_x/HC ratio has

TABLE 6

CHEMICAL KINETIC MODEL FOR HYDROCARBON/NITRIC OXIDE MECHANISM
(Stoichiometry imbalances may occur because of lumped parameter assumptions.)

Reaction	Model Values From Validation	Nominal Values for Propylene System[18]
(1) $h\nu + NO_2 \rightarrow NO + O$	0.4 min^{-1}	0.4 min^{-1}
(2) $O + O_2 + M \rightarrow O_3 + M$	1.32×10^{-5} $ppm^{-2}min^{-1}$	1.32×10^{-5} $ppm^{-2}min^{-1}$
(3) $O_3 + NO \rightarrow NO_2 + O_2$	40 $ppm^{-1}min^{-1}$	22-44 $ppm^{-1}min^{-1}$
(4) $O + HC \rightarrow 2RO_2$	6100 $ppm^{-1}min^{-1}$	6100 $ppm^{-1}min^{-1}$
(5) $OH + HC \rightarrow 2RO_2$	80 $ppm^{-1}min^{-1}$	244 $ppm^{-1}min^{-1}$
(6) $RO_2 + NO \rightarrow NO_2 + 0.5\ OH$	1500 $ppm^{-1}min^{-1}$	122 $ppm^{-1}min^{-1}$
(7) $RO_2 + NO_2 \rightarrow PAN$	6 $ppm^{-1}min^{-1}$	122 $ppm^{-1}min^{-1}$
(8) $OH + NO \rightarrow HNO_2$*	10 $ppm^{-1}min^{-1}$	99 $ppm^{-1}min^{-1}$
(9) $OH + NO_2 \rightarrow HNO_3$*	30 $ppm^{-1}min^{-1}$	300 $ppm^{-1}min^{-1}$
(10) $O_3 + HC \rightarrow RO_2$	0.0125 $ppm^{-1}min^{-1}$	0.00927 - 0.0125 $ppm^{-1}min^{-1}$
(11) $NO + NO_2 \rightarrow 2HNO_2$**	0.01 $ppm^{-1}min^{-1}$	
(12) $h\nu + HNO_2 \rightarrow NO + OH$	0.001 min^{-1}	
Additional reactions included in Model		
(13) $O_3 + NO_2 \rightarrow NO_3 + O_2$	.005 $ppm^{-1}min^{-1}$	.05 $ppm^{-1}min^{-1}$†
(14) $RO_2 + NO_3 \rightarrow PAN$	6 $ppm^{-1}min^{-1}$	122 $ppm^{-1}min^{-1}$

* Rate constant lumps third body concentration

** Water vapor lumped into rate coefficient

† Leighton,[17] p. 158

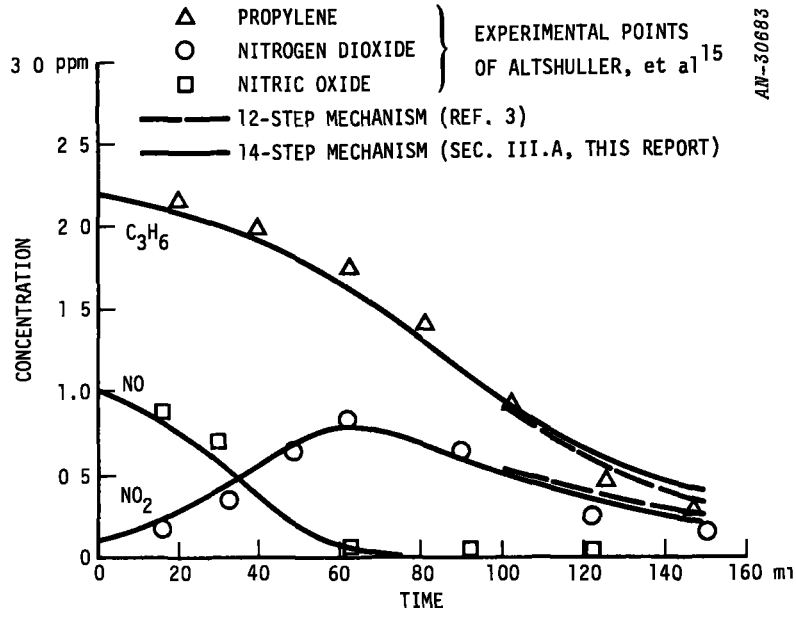

Figure 5. Computed Concentrations of Propylene, Nitric Oxide, and Nitrogen Dioxide Compared with Experimental Values

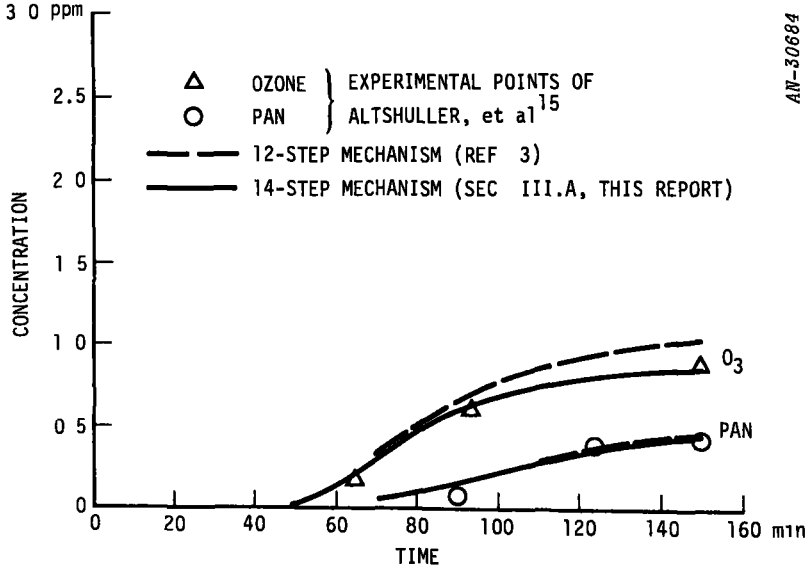

Figure 6. Computed Concentrations of Ozone and PAN Compared with Experimental Values

on the new model is the same as that reported in Ref. 3: ozone concentration decreases with increasing NO_x/HC ratio. The only difference is that, with the new model, the ozone levels are reduced by the additional removal mechanism.

B. CASES SELECTED FOR ATMOSPHERIC MODELING

1. Baseline Case

In order to provide a data base against which to compare the results of the atmospheric model, we selected a day during a smog episode, October 23, 1968. For this date, we used data recorded by Scott Research Laboratories[19] at Huntington Park. Because Huntington Park is centrally located in the Los Angeles Basin, its aerometric data is likely to reflect the effects of vehicular sources. This is an important consideration in this study. The day of October 23 was chosen for several reasons:

1. Readily available aerometric and meteorological data
2. The day is typical of high-oxidant, heavy-smog days in Los Angeles.
3. The prevalence of low wind speeds up to about 9:30 A.M. and the presence of a low inversion base (approximately 200 meters) indicate stable atmospheric conditions which lead to a worst-case approach in our computed results.
4. Previous modeling experience with this date[20]

2. Choice of Years

Four years were chosen for the cold-start vs hot-start comparison: 1968, 1971, 1974, 1980. The first year, 1968, has extensive atmospheric data used for validation as mentioned above, but the accuracy of the vehicular emission data base can only be classified as fair due to the large quantity of pre-1966 cars still on the road in 1968. By contrast, 1971 has the best and most reliable auto emissions data base of all the

years and it was chosen for this reason. The year 1974 was selected because it is the last model year before automotive emissions must satisfy the stringent 1975 standards. Thus for 1974, effects of the cold-start pulse are unlikely to be overshadowed by emissions from stationary sources. Finally, by 1980 over 70% of all car-miles in Los Angeles should be traveled by cars with 1975 or post-1975 emission controls. Hence 1980 was chosen because it is the year when the full impact of the 1975 auto emission standards is supposed to be felt.

3. Choice of Air Trajectory to Study Decentralization of Starts

The possibility has been suggested that a nonuniform spatial distribution of vehicle starts may reduce the effects of the cold-start contribution. To test this hypothesis, an air trajectory was selected that would traverse the Basin from West to East during the morning and early afternoon. The chosen trajectory passes over Downtown Los Angeles and ends in the eastern part of the San Fernando Valley. Figure 4 shows a diagram of the trajectory. The trajectory is typical for a September day which has low winds and stable atmospheric conditions. Using this trajectory we intend to compare the pollution levels for a single year under two different assumptions for the distribution of cold starts: a uniform and a nonuniform spatial distribution. The nonuniform distribution has been described in Sec. II A 2. The 1974 emissions data were used to generate source inputs for the trajectory.

C. ESTABLISHMENT OF BASELINE CASE

The baseline case was used successively to determine three critical parameters of the model:

1. The size of the diffusion coefficient
2. The scaling factor for the NO flux
3. The scale factor of the hydrocarbon rate constants

In addition, the base case was also used to ascertain the sensitivity of the CO buildup to the cold-start pulse and to generate the results reported in the next section.

1. Determination of Diffusion Coefficient

The functional dependence of the diffusion coefficient on height and wind speed has been described elsewhere.[21] Here we are concerned simply with the proper scaling of the entire diffusivity profile. This was accomplished by comparing the observed and computed buildup of carbon monoxide. Figure 7 shows the calculated and measured data. The upper solid curve was deemed to approach most closely the early-morning buildup prior to the onset of advection due to increasing horizontal wind speed. From 0600 to 0930 the wind speed is very low and the model essentially reproduces the CO buildup. The wind speed increase after 0930 and the model is no longer effective in estimating the CO concentration at a point.

Figure 7 also shows the sensitivity of the computed results both to a change in the value of diffusivity and to the removal of the cold-start contribution. Increasing the diffusivity by 50% causes the computed values to drop by several ppm. Removing the cold-start pulse causes an even more dramatic drop in the calculated early-morning buildup as well as a qualitative shape change in the curve.

2. Necessity for Scaling NO Flux

It has been observed in previous studies[2,20,21,22] that morning NO_x buildups do not fully account for the emitted NO obtained from source inventories. In other words, the nitrogen balance between inventories and measured NO_x concentrations is poor; sometimes it may be off by as much as a factor of four.[23] This has been shown to be true particularly on high-oxidant days such as October 23, 1968.[22] This phenomenon is not yet fully resolved, but it is speculated that gas-solid reactions may account for a large part of the discrepancy. This is known to be the case in smog chamber experiments, and recently Gay and Bufalini[24] have published experimental evidence supporting the existence of wall reactions which account for a major fraction of the nitrogen deficit.

Sec. III C
Fig. 7

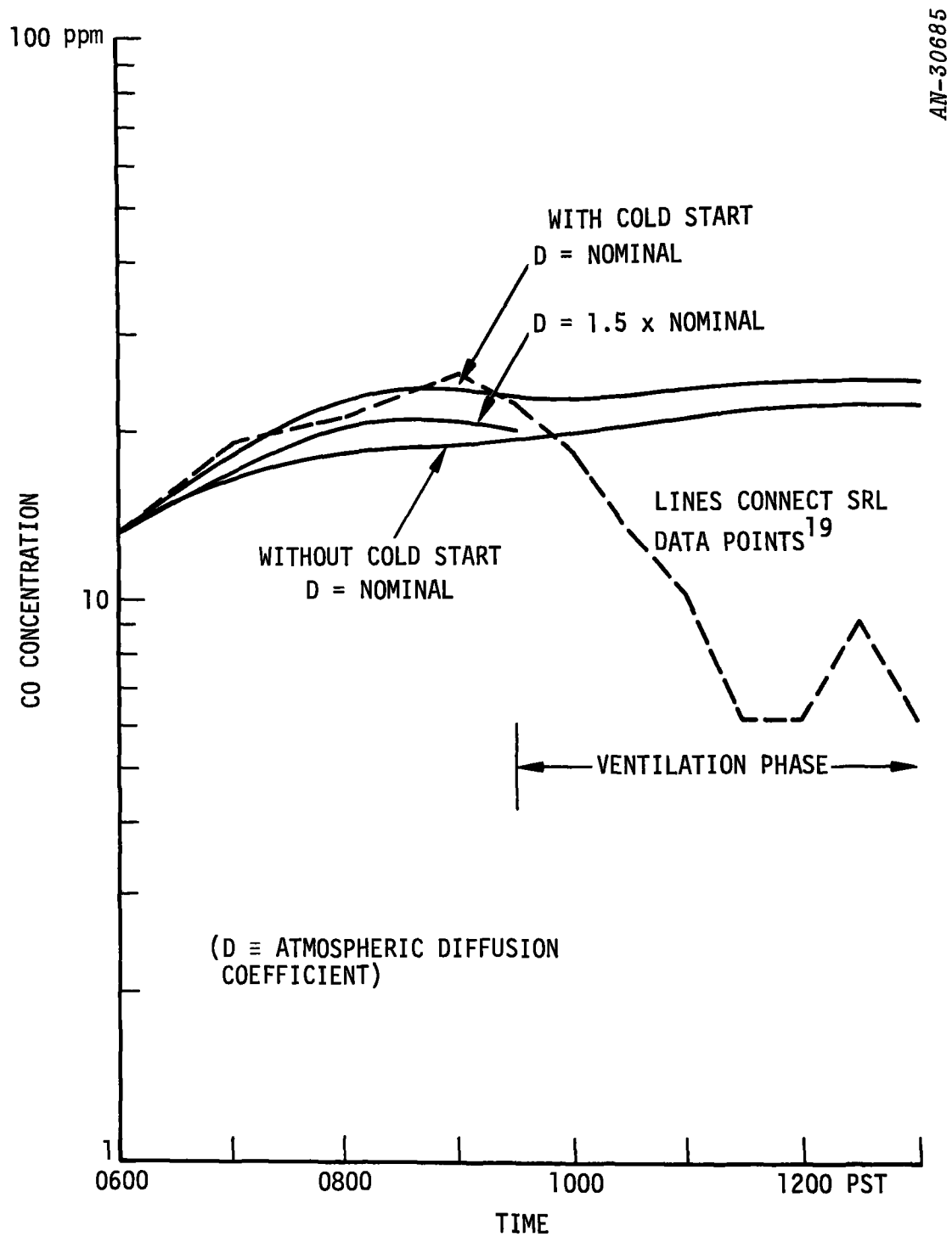

Figure 7. Influence of Cold Start and Diffusion Coefficient on Carbon Monoxide Buildup (See Text for Test Conditions)

Since the nitrogen imbalance involves rapid physical processes which are still not well defined, we resort to the expedient of artificially reducing the NO flux obtained from the source inventories in order to account for the NO_x losses during at least the early-morning buildup. In our particular case, which includes the cold-start contribution, scaling the NO flux by 1/4 yields satisfactory results. This is consistent with our previous work over the past few years.

3. Hydrocarbon Reactivity

It has been shown in earlier reports[22] that the reactivity of the hydrocarbon mixture in the atmosphere is generally lower than the reactivity of propylene by at least a factor of 2. It is thus necessary to adjust the rate constants of the reactions involving hydrocarbons since the validation of the kinetic model was done for a propylene system. Using the rates shown in Table 6 results, as expected, in the production of amounts of ozone which are far larger than the atmospheric measurements indicate. Our experience has shown that adjustment of the hydrocarbon rate constants by about 1/3 to 1/2 the propylene values yields ozone concentrations consistent with aerometric data.

For the case of October 23, 1968, we have determined that a 1/3 rate adjustment is necessary to obtain the correct ozone concentration. Further details on testing other values of the rate constants can be found in Ref. 20.

4. Summary of Steps Required to Establish the Baseline Case

In establishing the baseline case, the following steps were taken:

1. Determination of the diffusion coefficient using the CO buildup in the morning
2. Decreasing the NO flux by 1/4 to achieve the nitrogen balance
3. The rate constants of the hydrocarbon reactions were multiplied by 1/3 to simulate the lower reactivity of the atmospheric hydrocarbon mixture (as indicated by gas chromatographic data[16,19]), thus producing the correct amounts of ozone.

Figures 7 to 11 show comparisons of the computed results with the atmospheric measurements collected by Scott Research Laboratories.[19] The carbon-monoxide modeling in Fig. 7 was discussed in Sec. III C 1, and the other figures show the reactive pollutants. The NO (shown in Fig. 8) follows the data rather accurately, whereas the NO_2 (shown in Fig. 9) lags behind the measured data. The time lag is the result of lowering the hydrocarbon rates coupled with the omission in this simulation of the ventilation phase. It seems paradoxical that the NO should show such good correspondence with the data but that for NO_2 the agreement is poorer. One possible explanation of this effect is that for NO fast chemical reactions coupled with vertical diffusion tend to minimize the susceptibility of NO to advection. By contrast, it is well known that the residence time of NO_2 over an urban area is much longer, and NO_2 is thus highly sensitive to advective forces.

Time lags can also be seen in Figs. 10 and 11 for ozone and reactive hydrocarbon, respectively. The ozone buildup is reproduced quite well by the model, but the model fails to agree with the measured ozone decay. Again, fast chemical reactions can account for the ozone buildup. The decay of ozone via chemical reactions is relatively slow, thus ozone decay at the point modeled is the result of ventilation. For reactive hydrocarbon, the buildup during the stagnation phase (0600-0930) is well reproduced, but the decay is chemically very slow and advection is the dominant effect.

Sec. III C
Figure 8

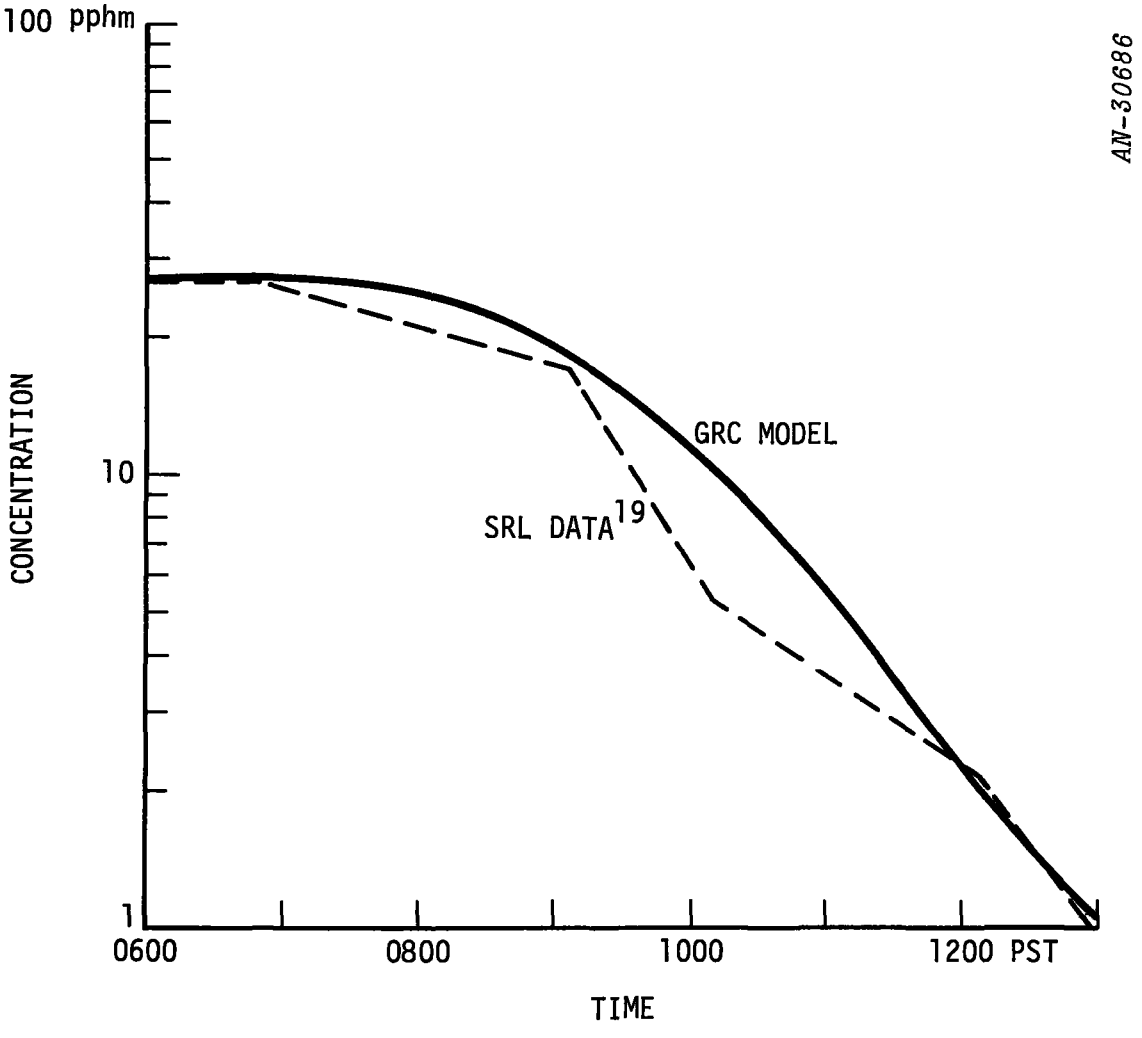

Figure 8. Ground Level Nitric Oxide Concentration on October 23, 1968 in the Central Los Angeles Basin

Sec. III C
Figure 9

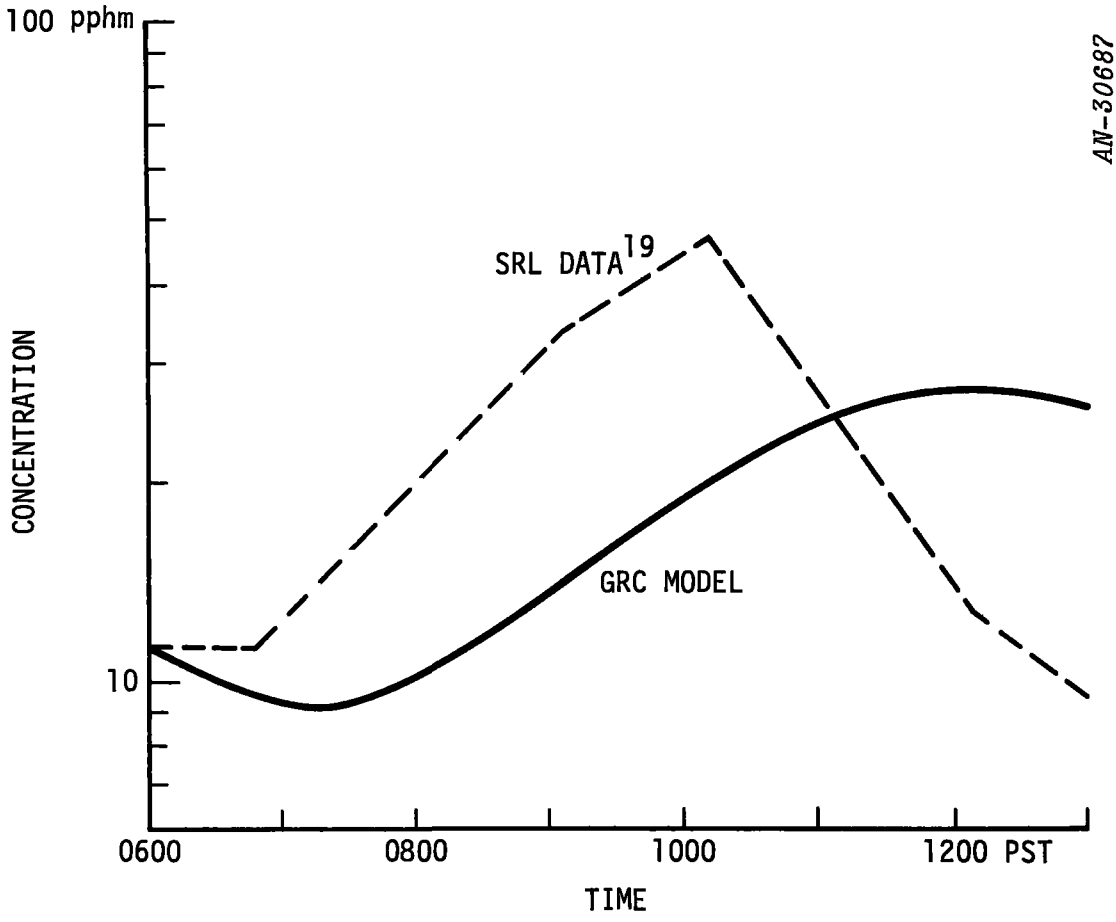

Figure 9. Ground Level NO_2 Concentration on October 23, 1968 in the Central Los Angeles Basin

Sec. III C
Figure 10

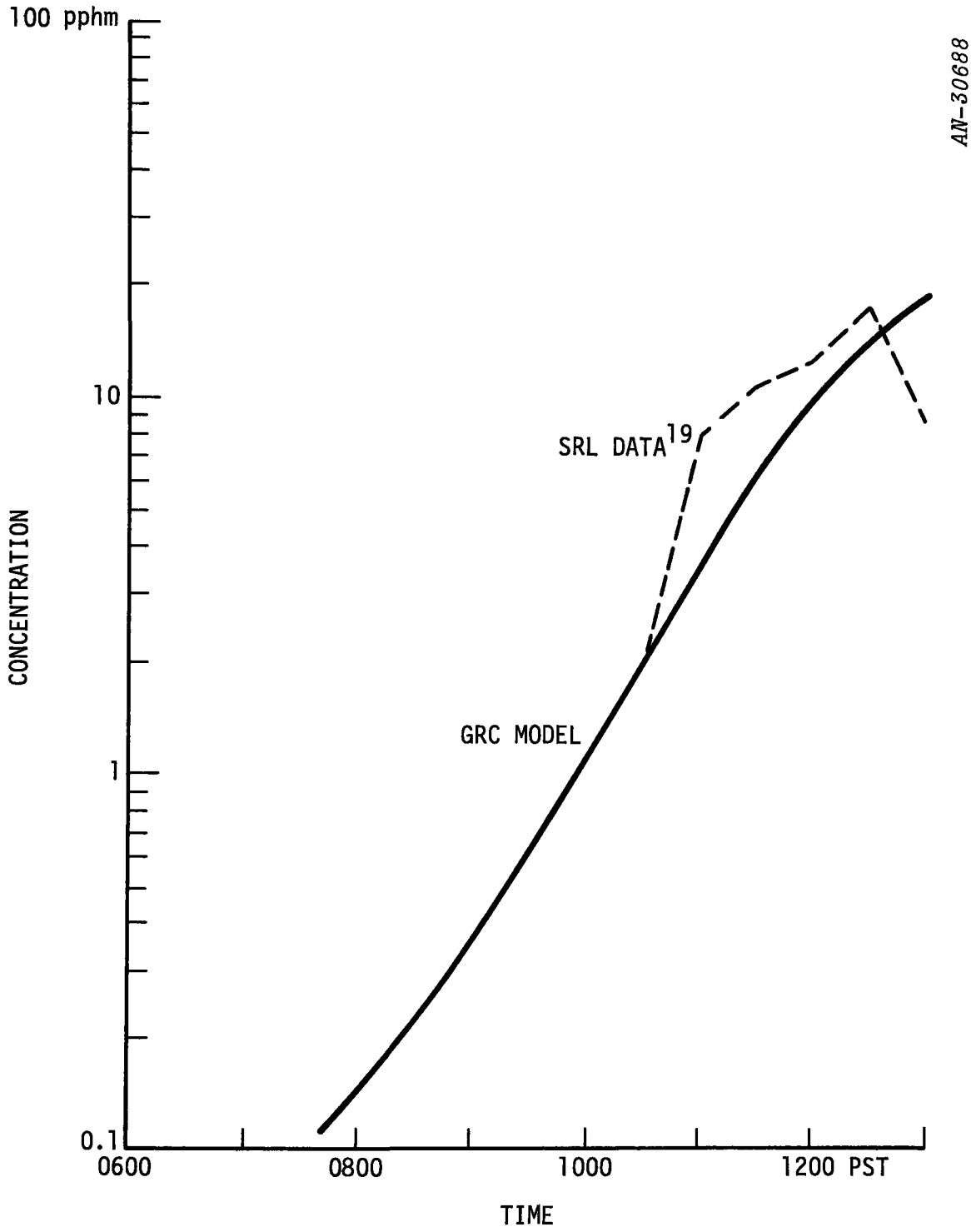

Figure 10. Ground Level Ozone Concentration on October 23, 1968 in the Central Los Angeles Basin

Sec. III C
Figure 11

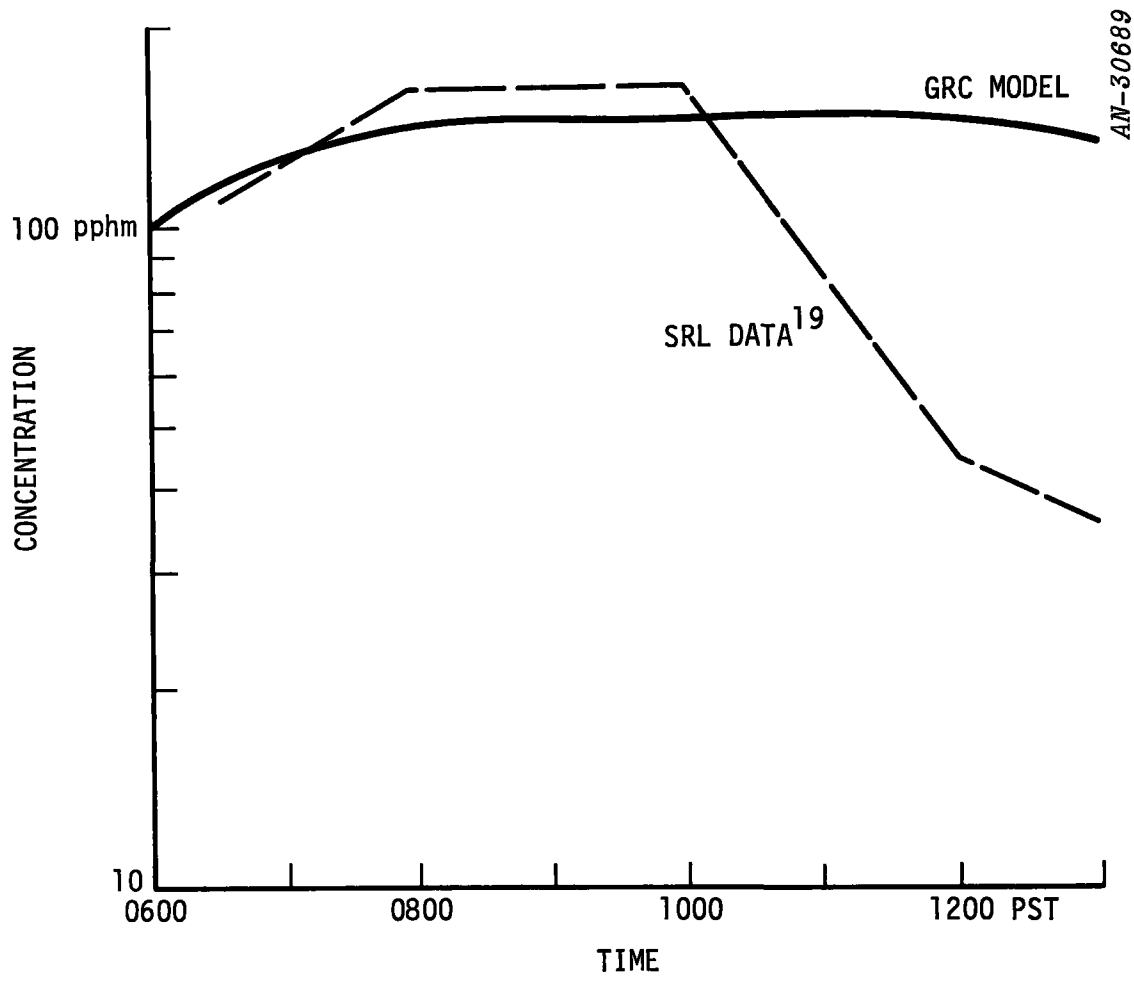

Figure 11. Ground Level Reactive Hydrocarbon Concentration on October 23, 1968 in the Central Los Angeles Basin

Sec. IV A
Table 7

IV. TEST RESULTS FOR DETERMINING COLD-START EFFECTS

A. RESULTS UNDER STAGNANT ATMOSPHERIC CONDITIONS

The contribution of cold-start emissions to air pollution was determined for a location in the central Los Angeles basin on a day characterized by very light winds. Concentration histories of various pollutants were computed, both with and without the morning vehicle start-up emissions in the 0600-0900 hour time interval.

The effect of cold-start emissions of NO , CO , and reactive hydrocarbon on atmospheric loading during the early morning hours is demonstrated in Table 7 in the form of emissions ratios for the 25-square-mile test region; i.e., ratios of emissions with cold-start to emissions without cold start.

TABLE 7

EMISSION EFFECTS

(Ratios of emissions with cold-start to emissions without cold-start, each for 0600-0900 time interval in central L.A. basin)

Species	Year			
	1968	1971	1974	1980
NO	1.153	1.157	1.156	1.009
CO	1.479	1.568	1.526	2.297
Reactive hydrocarbon	1.077	1.103	1.105	1.107

To show the effect of cold-start emissions on ambient air quality, we have computed concentration ratios for two product pollutants, ozone and nitrogen dioxide, and for carbon monoxide. Shown in Table 8, the ratios are ground concentration with cold-start divided by ground concentration

without cold-start, taken at 1300 hours (the end of the simulation run) for O_3 and NO_2, and at peak concentration (whenever it occurs) for CO.

TABLE 8

AIR QUALITY EFFECTS

(Ratios of concentration with cold-start to concentration without cold-start in central L.A. basin)

Time	Species	Year 1968	1971	1974	1980
1300 hours	O_3	1.024	1.028	1.014	1.071
1300 hours	NO_2	1.011	1.015	1.014	1.002
Peak	CO	1.093	1.132	1.127	(no peak)

Table 9 combines carbon monoxide data from Tables 7 and 8 with the addition of the CO emissions ratio for the 0600-1300 time period. Two features of these data are notable; first, cold-start contributions to

TABLE 9

CARBON MONOXIDE EFFECTS

(Figures shown are ratios for quantities with cold-start to quantities without cold-start)

	Year 1968	1971	1974	1980
0600-0900 Emissions	1.479	1.568	1.526	2.297
0600-1300 Emissions	1.216	1.257	1.238	1.586
Peak Concentration	1.093	1.132	1.127	(no peak)

total CO emissions are considerable, even when taken over the complete 7-hour span of the simulation; and second, in spite of a sizeable increase in CO emissions in the relatively short vehicle start-up period, only modest increases in peak CO concentration are seen, giving us a measure of the mitigating effects of atmospheric dispersion and dilution on non-reacting species.

B. RESULTS OF CROSS-BASIN TRAJECTORY ANALYSIS

To determine the effect of a suburb-oriented cold-start distribution, the moving air parcel model was employed to compute various pollutant concentrations along a cross-basin trajectory typical of September wind patterns (see Sec. II C 2). Using 1974 emissions data, two cold-start geographical distributions were simulated, one uniform and one weighted 3-to-1 between the suburbs and downtown (see Sec. II A 2).

The cold-start contributions to pollutant loading in the air parcel are shown in Table 10 as the ratios of emissions with cold-start to emissions without cold-start for NO , CO , and reactive hydrocarbons. Note that the decentralized start distribution loads the air parcel with more pollutants than the uniform one because of relatively high morning exposure of the air parcel to areas away from the basin center.

TABLE 10

EMISSION EFFECTS FOR 1974 TRAJECTORY

(Ratios of emissions with cold-start to emissions without cold-start, each for 0600-0900 time interval)

Species	Spatially Uniform Start Distribution	Decentralized Start Distribution
NO	1.168	1.183
CO	1.546	1.594
Reactive Hydrocarbon	1.134	1.146

Sec. IV B
Table 11

The effect of vehicle start distribution on air quality in the air parcel may be seen in Table 11 by comparing the concentration ratios computed for the uniform and decentralized start distributions. These concentration ratios (ground concentration with cold-start to ground concentration without cold-start) were computed at peak value for CO , and at the end of the air-trajectory (1400 hours) for the chemical product pollutants O_3 and NO_2 .

TABLE 11

AIR QUALITY EFFECTS FOR 1974 TRAJECTORY

(Ratios of concentration with cold-start to concentration without cold-start)

Time	Species	Spatially Uniform Start Distribution	Decentralized Start Distribution
1400 hours	O_3	1.039	1.042
1400 hours	NO_2	1.024	1.026
Peak	CO	1.125	1.136

Finally, as in the previous section, we compare the contributions of cold-start CO emissions to total CO emissions, and to the resultant peak concentrations of CO in the air parcel (see Table 12). (The 0600-1400 time period is the complete duration of the simulated trajectory.) As before, the noteworthy features of these data are the considerable size of the cold-start emission contributions, and the weakness of the coupling between emissions and air quality effects for a non-reacting species.

Sec. IV B
Table 12

TABLE 12

CARBON MONOXIDE EFFECTS FOR 1974 TRAJECTORY

(Figures shown are ratios for quantities with cold-start to quantities without cold-start)

	Spatially Uniform Start Distribution	Decentralized Start Distribution
0600-0900 Emissions	1.546	1.594
0600-1400 Emissions	1.250	1.273
Peak Concentration	1.125	1.136

V. CONCLUDING REMARKS

A. INTERPRETATION OF MODELING RESULTS

Considering the wide variety of emission sources and control measures we find that the pollution input of cold starts can be very large or very small as shown in Table 7. Its nitric oxide contribution (between 6 and 9 A.M.) stays near 15% of all emissions until the end of the present decade, when it drops below one percent. Dominant effects of stationary sources compared with vehicles cause this sharp decrease. Reactive hydrocarbon starting emissions comprise about 10% of the 6 to 9 A.M. inputs. Because of choked engine operation, carbon monoxide starting contributions range from 48% to 130% of running CO emissions during the morning traffic peak hours.

It is of central interest here to examine the incremental change in air pollution due to the vehicle starting process. As illustrated in Table 8, 1300-hour levels of oxidant species, O_3 and NO_2, are only raised by a few percent. Apparently, the reaction times to produce these compounds are long enough to allow considerable atmospheric dilution. Carbon monoxide is treated as nonreactive in the simulations and it is more strongly affected than the oxidant species. Because carbon monoxide is emitted directly and oxidant is not, it may be more meaningful to use the emission ratios (Table 7) instead of the air quality ratios (Table 8) for setting standards. This procedure would more nearly reflect the increased exposure of receptors in the area where the cars are started.

Expressed as percentages, cold-start emissions (Table 7) exhibit a long-term upward trend. This tendency is attributable to lower running emissions achieved by more sophisticated control systems, accompanied by thermal inertia in catalytic devices, which aggravates the cold start problem in advanced systems. The oxides of nitrogen actually assume a lesser role as time goes on because they pose less of a cold-start control problem than do the other contaminants. NO_x compounds are also

special in that stationary inputs are projected to grow significantly over a period when vehicles are experiencing more stringent controls.

Tables 7 through 9 demonstrate that the time phasing of vehicle activities and reactions influences the morning startup effects. The relatively high deposition rates in the 6 to 9 A.M. time interval have these effects superimposed on them. Spreading the averaging period over the 6 A.M. to noon time interval reduces the relative fractional contribution. Although it was not modeled, delaying the startup time and the traffic peak would also drive downward the air pollution levels, because higher wind speed and surface heating would enhance the dispersion.

Spatial distribution of cold-starts was also investigated in the study. An air trajectory, going from the western Los Angeles basin over the downtown area and up into Burbank, was chosen. Essentially no difference was noted between one case with uniformly distributed cold-starts and another case with three times the cold-start density at the coast as that in downtown (Tables 10-12). This lack of sensitivity to spatial distribution occurred for all pollutants for the 0600-1400 time interval covered by the trajectory.

B. SOME ALTERNATIVES FOR WEIGHTING FACTORS TO COMBINE COLD-START AND HOT-START CYCLE TEST RESULTS

It is clear from the results previously discussed that cold-start emissions cannot be neglected in setting automotive emission standards. The question is, how should the emissions be weighted to reflect the relative influences of cold and hot starts? We now examine some alternative weighting methods.

Based on our analyses, three possible methods might be considered:

1. Air Quality Method
2. Vehicle Activities Method
3. Emissions Method

Each of these is related in some way to the morning emissions in contrast with all-day averaging. The objective of each method is to obtain a weighting factor w for the formula

$$E_w = wc + (1-w)h$$

in which E_w = weighted average of cold and hot-start cycle emissions
c = cold-start cycle emissions
h = hot-start cycle emissions
w = cold-start weighting factor

The air quality method uses our simulation results summarized in Tables 7 and 8. It is the ratio of percentage deterioration in air quality to percentage increased emissions. If, for example, a five-percent contaminant concentration increase is caused by a ten-percent emission increase (due to cold-start), then $w = 0.5$ by the air quality method. This method accounts for the leverage factor of emissions upon air quality. A problem arises in determining the percentage deterioration in air quality due to secondary pollutants such as NO_2 and O_3 since no simple cause/effect relationship exists between these pollutants and their precursors, NO and HC (reactive). We chose to average between the percentage increases in pollution level due to NO_2 and O_3, and similarly, to average between HC (reactive) and NO emission percentages to get the emission term in the denominator.

From Table 7, we find that the average NO and HC (reactive) percentage emission increase for 1971 is 13%. Similarly, from Table 8 we obtain an average increase of 2.15% for $(NO_2 + O_3)$. This yields a value of $w = 2.15/13 = 0.17$. The relatively low value of w reflects the dilution which occurs during the reaction phase. Applying the procedure to CO in a straightforward manner, one obtains $w = 0.23$. The larger weighting factor for CO arises because it is not considered to be reactive. The air quality method results are summarized in Table 13.

Sec. V B
Table 13

TABLE 13

WEIGHTING FACTORS FOR AIR QUALITY METHOD FOR 1971

Pollutant	w
Reactive	0.17
CO	0.23

The vehicle activities method is based on vehicle-miles per cold start during the morning hours. Let

$$a = \frac{\text{(mileage per vehicle during time period)}}{\text{(cold-starts per vehicle during time period)}}$$

Then this method gives w from the following formulas

$$w = \frac{7.45}{a} \quad ; \text{ for } a > 7.45$$

$$w = 1 \quad ; \text{ for } a \leq 7.45$$

because the driving cycle covers 7.45 miles of operation. Driving patterns for Los Angeles obtained from Ref. 1 (page 1-45) show that for the 0600-0900 time period, the average trip length is 10.6 miles. Hence, $a = 10.6$ and $w = 0.70$. Likewise, for the interval 0600-1200 we find $a = 12.5$, and hence, $w = 0.60$. (Note that this method does not differentiate between reactive and nonreactive emissions.) These results are summarized in Table 14.

The third method, the emissions method, simply reduces the cold-start weighting factor obtained from the vehicle activities method to account for stationary source background emissions. The reduction is accomplished by applying a scale factor that is the ratio of vehicular

TABLE 14

WEIGHTING FACTORS FOR VEHICLE-ACTIVITIES AND EMISSIONS METHODS

Method	Time Period	Type of Emissions	
		(HC + NO)	CO
Vehicle Activities	0600-0900	0.70	0.70
	0600-1200	0.60	0.60
Emissions*	0600-0900	0.52	0.70
	0600-1200	0.43	0.60

*Central L.A. Basin location. Emissions used are for 1971. Stationary CO emissions are considered to be negligible.

emissions to total emissions for the same time period used in the activities method. It should be noted that in this method the scale factor used to multiply w will in general be a function of geographical location, since the ratio of vehicular to stationary emissions is not constant throughout an urban area. However, average total emissions for an urban area could be used. Another possibility is to follow a worst-case approach and choose the geographical region with the highest vehicular/stationary emissions ratio. For illustrative purposes, we have computed scale factors for reactive emissions (HC + NO) and for CO for the central L.A. Basin location used throughout the study. These calculations require hourly average emissions data for the various sources. We used those for 1971. Table 14 summarizes the results obtained for the vehicle-activities and emissions methods.

Finally, to illustrate how the incorporation of cold-start emissions on a weighted basis would affect the emissions rating of an average 1971

car, we have computed some sample weighted emission factors. The range of w's shown in Tables 13 and 14 is 0.17 - 0.70 for the reactive pollutants (HC and NO) and 0.23 - 0.70 for CO . Table 15 contains the running emission factor for each pollutant and the range of corrected emission factors associated with use of the lower and upper values of w for that pollutant.

TABLE 15

AVERAGE 1971 VEHICLE EMISSION FACTORS ADJUSTED TO ACCOUNT FOR MORNING COLD-START EFFECTS

	Running Emission Factor (w = 0)	$w = w_{min}$	$w = w_{max}$
NO_x, gm/mi	3.71	3.83	4.21
HC, gm/mi	2.80	2.94	3.38
CO, gm/mi	29.66	32.52	38.36

The choice of weighting method rests on the air quality objective of the control program. The vehicle activities method, which is the most stringent of these three for morning emissions, would be used for protection against excessive roadside CO exposure. On the other hand, the air quality method might be applied to the reactive pollutants to reflect the yield factors and dilution factors affecting photochemical pollutants. If the morning hydrocarbon air quality standard is imposed on photochemically active pollution, however, the emissions method might be most satisfactory. Clearly, the selection of approach is influenced by the direction taken in making policy in air pollution abatement. The choice of method, therefore, is not easily amenable to analysis.

REFERENCES

1. D. H. Kearin and R. L. Lamoureaux, A Survey of Average Driving Patterns in the Los Angeles Urban Area, System Development Corporation TM-(L)-4119/000/01, February 28, 1969.

2. A. Eschenroeder and J. R. Martinez, Mathematical Modeling of Photochemical Smog, General Research Corporation IMR-1210, December 1969.

3. A. Eschenroeder and J. R. Martinez, Further Development of the Photochemical Smog Model for the Los Angeles Basin, General Research Corporation CR-1-191, March 1971.

4. P. L. Hanst, "Mechanism of Peroxyacetyl Nitrate Formation," Journal of the Air Pollution Control Association, Vol. 21, No. 5, May 1971, pp. 269-271.

5. P.J.W. Roberts, P.M. Roth, and C.L. Nelson, "Contaminant Emissions in the Los Angeles Basin--Their Sources, Rates, and Distribution," Appendix A of Development of a Simulation Model for Estimating Ground Level Concentrations of Photochemical Pollutants, Systems Applications, Inc., Report 71SAI-6, March 1971.

6. Air Pollution Control in California; 1970 Annual Report, Air Resources Board, January 1971.

7. Profile of Air Pollution Control in Los Angeles County, Air Pollution Control District, County of Los Angeles, January 1969.

8. T. Huls, Environmental Protection Agency, Air Pollution Control Office, Private Communication, May 18, 1971.

9. M. J. McGraw and R. L. Duprey, Air Pollutant Emission Factors (Preliminary Document), U.S. Environmental Protection Agency, April 1971, p. 24.

10. "DHEW Urban Dynamometer Driving Schedule," The Federal Register, Vol. 35, No. 219, Part II, November 10, 1970, Appendix A, p. 17311.

11. "Test Procedures, Emission Standards Revised," California Air Resources Board Bulletin, Vol. 2, No. 9, Nov.-Dec. 1970, p. 4.

12. Gasoline Modification; Its Potential as an Air Pollution Control Measure in Los Angeles County, A Joint Project by California Air Resources Board, Los Angeles County APCD, and Western Oil and Gas Association, November 1969, p. 28.

13. A. J. Hocker, California Air Resources Board, Private Communication, May 19, 1971.

14. M. Neiburger and J. G. Edinger, Meteorology of the Los Angeles Basin with Particular Respect to the "Smog" Problem, Air Pollution Foundation Report No. 1, April 1954.

15. A. P. Altshuller, S. L. Kopczynki, W. A. Lonneman, T. L. Becker, and R. Slater, "Chemical Aspects of the Photooxidation of the Propylene-Nitrogen Oxide System," Environmental Science and Technology, Vol. 1, No. 11, Nov. 1967, pp. 899-914.

16. Atmospheric Reaction Studies in the Los Angeles Basin, Vols. I - IV, Scott Research Laboratories, February 1970.

17. P. A. Leighton, Photochemistry of Air Pollution, N.Y.: Academic Press, 1961.

18. K. Westberg and N. Cohen, The Chemical Kinetics of Photochemical Smog as Analyzed by Computer, AIAA Third Fluid and Plasma Dynamics Conference Paper No. 70-753, Los Angeles, June 29-July 1, 1970.

19. Final Report on Phase I, Atmospheric Reaction Studies in the Los Angeles Basin, Vol. I and II, Scott Research Laboratories, June 30, 1969.

20. A. Q. Eschenroeder and J. R. Martinez, A Modeling Study to Characterize Photochemical Atmospheric Reactions in the Los Angeles Basin Area, General Research Corporation CR-1-152, Nov. 1969.

21. A. Q. Eschenroeder and J. R. Martinez, Concepts and Applications of Photochemical Smog Models, General Research Corporation TM-1516, June 1971.

22. A. Q. Eschenroeder and J. R. Martinez, Analysis of Los Angeles Atmospheric Reaction Data from 1968 and 1969, General Research Corporation CR-1-170, July 1970.

23. R. Gordon, H. Mayrsohn, R. Ingels, "C_2-C_5 Hydrocarbons in the Los Angeles Atmosphere," Environmental Science and Technology, Vol. 2, pp. 1117-1120, Dec. 1968.

24. B. W. Gay and J. J. Bufalini, "Nitric Acid and the Nitrogen Balance of Irradiated Hydrocarbons in the Presence of Oxides of Nitrogen," Environmental Science and Technology, Vol. 5, No. 5, May 1971, pp. 422-425.